

Investigation of Microstructure and Mechanical Properties of ECAP-Processed AM Series Magnesium Alloy

K.R. Gopi, H. Shivananda Nayaka, and Sandeep Sahu

(Submitted March 24, 2016; in revised form June 27, 2016; published online July 19, 2016)

Magnesium alloy Mg-Al-Mn (AM70) was processed by equal channel angular pressing (ECAP) at 275 °C for up to 4 passes in order to produce ultrafine-grained microstructure and improve its mechanical properties. ECAP-processed samples were characterized for microstructural analysis using optical microscopy, scanning electron microscopy, and transmission electron microscopy. Microstructural analysis showed that, with an increase in the number of ECAP passes, grains refined and grain size reduced from an average of 45 to 1 μm. Electron backscatter diffraction analysis showed the transition from low angle grain boundaries to high angle grain boundaries in ECAP 4 pass sample as compared to as-cast sample. The strength and hardness values showed increasing trend for the initial 2 passes of ECAP processing and then started decreasing with further increase in the number of ECAP passes, even though the grain size continued to decrease in all the successive ECAP passes. However, the strength and hardness values still remained quite high when compared to the initial condition. This behavior was found to be correlated with texture modification in the material as a result of ECAP processing.

Keywords AM70 alloy, equal channel angular pressing (ECAP), grain refinement, microstructural analysis, mechanical properties, severe plastic deformation (SPD)

1. Introduction

Magnesium (Mg) and its alloys are considered as structural material in industrial applications due to their properties like low density, good castability, high specific strength, and low cost. The requirement of magnesium alloys is more toward industrial applications, particularly aerospace and automotive industries (Ref 1, 2). The main limitation into their industrial application is the poor room temperature formability due to their hexagonal closed packed (HCP) structure. Formability at room temperature in Mg alloys can be improved by grain refinement in the microstructure as fine-grained Mg alloy possesses better ductility as well as lower ductile to brittle transition temperature (DBTT) (Ref 3). The grain refinement can easily be achieved by severe plastic deformation (SPD) techniques (Ref 4-8). Equal channel angular pressing (ECAP) is one of the simple and most effective methods of SPD to improve the material properties (Ref 9, 10). ECAP is a process in which the workpiece is subjected to shear deformation and thus, severe plastic strain is induced into the material without any change in the cross-sectional dimension of the sample. Feature like microstructure has a

major effect on the mechanical properties (Ref 11). ECAP process leads to ultrafine-grained microstructure in the material which may show superplastic deformation at low temperature and high strain rate. In HCP-structured metals, grain refinement also leads to textural changes, i.e., high strengthening in some particular directions. Magnesium alloys are usually Mg-Al system where aluminum addition improves the mechanical property as well as the castability. Addition of aluminum up to 6% and more makes the alloy age-hardenable. Manganese (Mn) addition plays a vital role in grain refinement for magnesium alloys. Aluminum-manganese (AM) series magnesium alloys are widely used in manufacturing various automobile components such as seat frame, instrument panels, etc., due to their better damping, toughness, impact absorption, and elongation properties compared to aluminum-zinc (AZ) series alloys (Ref 12).

Some ECAP works were carried out on various magnesium alloys with different designs of ECAP die in order to investigate the modification in microstructure and mechanical properties as a result of ECAP processing. Kulyasova et al. carried out ECAP on AM60 magnesium alloy to enhance its fatigue endurance limit (Ref 13). Akbaripanah et al. processed extruded AM60 magnesium alloys by ECAP with internal die angle (Φ) of 90° and outer radius (Ψ) of 20° at the intersection using route B_C at 220 °C up to 6 passes (Ref 14). It was observed that, ECAP influenced both, grain size and texture and the process improved strength as well as ductility of AM60 magnesium alloy. In another work by Akbaripanah et al., the same ECAP processing was shown to improve AM60 magnesium alloy's fatigue properties (Ref 15). Dumitru et al. studied the ECAP processing on ZK60 magnesium alloy and showed that ECAP processing led to reduction of grain size, improvement its ductility, as well as a transition from brittle to ductile behavior (Ref 16).

In spite of various applications of AM series magnesium alloy, limited work has been done to improve the physical

K.R. Gopi and **H. Shivananda Nayaka**, Department of Mechanical Engineering, National Institute of Technology Karnataka, Surathkal 575025, India; and **Sandeep Sahu**, Department of Materials Science and Engineering, Indian Institute of Technology Kanpur, Kanpur 208016, India. Contact e-mails: me14f04.gopi@nitk.edu.in, hsn_mech@nitk.ac.in, and ssandy@iitk.ac.in.

properties of AM series magnesium cast alloys. Since AM series magnesium alloys possess better damping, elongation, and impact absorption properties, we may further improve these properties by using ECAP so that its application can be expanded in different areas of engineering. Also, not much work on AM70 cast alloy by ECAP processing is reported. The aim of the present work is to investigate the role of ECAP processing on AM70 cast alloy in modifying its microstructure and mechanical properties. For it, ECAP die with channel angle (Φ) as 110° and outer arc of curvature (Ψ) as 20° using route B_C was used to process AM70 magnesium alloy. The developments of microstructure, hardness, and tensile properties, i.e., ultimate tensile strength (UTS), yield strength (YS), and ductility, were investigated.

2. Material and Experimental Procedure

AM70 (Mg-7.1Al-0.35Mn) magnesium alloy cast billets of dimension $240 \text{ mm} \times 100 \text{ mm} \times 24 \text{ mm}$ were machined to produce cylindrical samples of diameter 15.8 mm and length 95 mm. These samples were subjected to ECAP processing using a special type of split die (as shown in Fig. 1a) having two intersecting channels at internal die angle (Φ) of 110° and outer arc of curvature (Ψ) of 20° . ECAP split die parts were fabricated from hot die steel (HDS) and held together using six large bolts. Pressing was carried out using universal testing machine (UTM) as shown in Fig. 1(b). Prior to ECAP processing, machined samples were homogenized at 400°C for 24 h in a muffle furnace in order to make sure that the constituents are distributed uniformly within the matrix. Homogenized samples were subjected to ECAP at 275°C using route B_C at a speed of 1 mm/s, in which the samples were rotated by 90° between 2 successive passes, every time in the same direction. Before pressing, ECAP die was uniformly heated at 275°C using six electrical resistance heaters which were placed inside the vertical channels in the die. The temperature was measured using a thermocouple which was inserted at the intersection point of the ECAP die channels. Temperature was stabilized using a temperature controller and it was continuously monitored during the ECAP processing. Homogenized sample was placed in the die for 20 min in order to attain the required temperature before pressing. Molybdenum disulfide (MoS_2) was used as a lubricant to avoid frictional losses. Samples were pressed using a plunger to produce an equivalent strain of 0.8, according to the equation (Ref 9),

$$\varepsilon = \frac{1}{\sqrt{3}} \left\{ 2 \cot \left(\frac{\phi}{2} + \frac{\psi}{2} \right) + \psi \cos ec \left(\frac{\phi}{2} + \frac{\psi}{2} \right) \right\}, \quad (\text{Eq 1})$$

where ε is the total strain, Φ is the die channel angle, and Ψ is the outer arc of curvature.

During the successive passes, the samples were rotated by 90° , every time in the same direction followed by pressing. The above-mentioned process was performed up to 4 passes. The as-cast, homogenized, and ECAP-processed samples were prepared for microstructural analysis. Sample preparation involved sequential mechanical polishing using various emery papers of grit size 400-2000 followed by cloth polishing using $0.05 \mu\text{m}$ Al_2O_3 as an abrasive material. All polished samples were etched using picral acetate (4.2 g picric acid, 50 ml ethanol, 20 ml acetic acid, and 20 ml distilled water), washed with ethanol, and finally dried with forced air in order to reveal grain boundaries. Samples

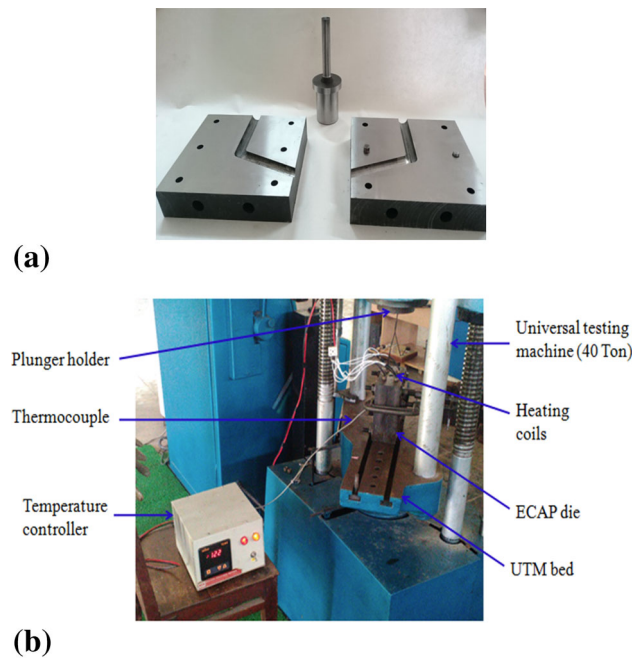


Fig. 1 (a) ECAP die with plunger (b) UTM with ECAP setup

for microstructural observation were prepared in a direction perpendicular to the direction of pressing. Microstructural analysis of the samples was performed using optical microscopy (OM), scanning electron microscopy (SEM, JEOL JSM-6380LA), and transmission electron microscopy (TEM, JEOL JEM-2100). Grain size was estimated using linear intercept method. Microstructure of the samples was also analyzed by orientation imaging microscopy (OIM)-based electron backscatter diffraction (EBSD) technique using Oxford Instruments 'Nordlys' detector attached to field emission scanning electron microscope (JEOL JSM-7100F) for revealing grain structure, grain orientation, and grain boundaries misorientation angles. For EBSD analysis, the mechanically polished samples were also electro-polished in order to minimize the damage caused by mechanical polishing. The electro-polishing was performed using Struers' standard AC2 electrolyte at 16 V for 80 s at -30°C . EBSD was carried out at 20 kV voltage and working distance of 17 mm. The step size was kept as 0.25 and $0.5 \mu\text{m}$. HKL Channel 5 software was used to analyze the acquired EBSD data. X-ray diffraction (XRD) was conducted to identify different phases present in the samples. XRD technique was conducted with a computer-controlled diffractometer fitted with Ni filter which was operated at 30 kV voltage and 20 mA current with $\text{Cu}\alpha$ radiation. The diffraction angle (2θ) range was given from 20° to 90° at a scan speed of $2^\circ/\text{min}$. Also, the mechanical properties of the samples were tested using tensile test. For this, cylindrical dog-bone tensile specimens of gage length 16 mm were prepared as per ASTM-E8 standard. Tensile test was performed at room temperature using Shimadzu AG-X plus™ 100 kN universal testing machine (UTM) with a steady cross-head speed of 0.25 mm/min. Omni-tech microhardness tester, fitted with Vickers indenter, was used to carry out hardness test by applying a load of 25 gram and dwell time of 15 s. Indentations were taken at equal intervals on the middle area of the sectioned region in each of the ECAP-processed samples in order to avoid any irregularity that might be taking place due to deformation near head and tail regions of the processed samples.

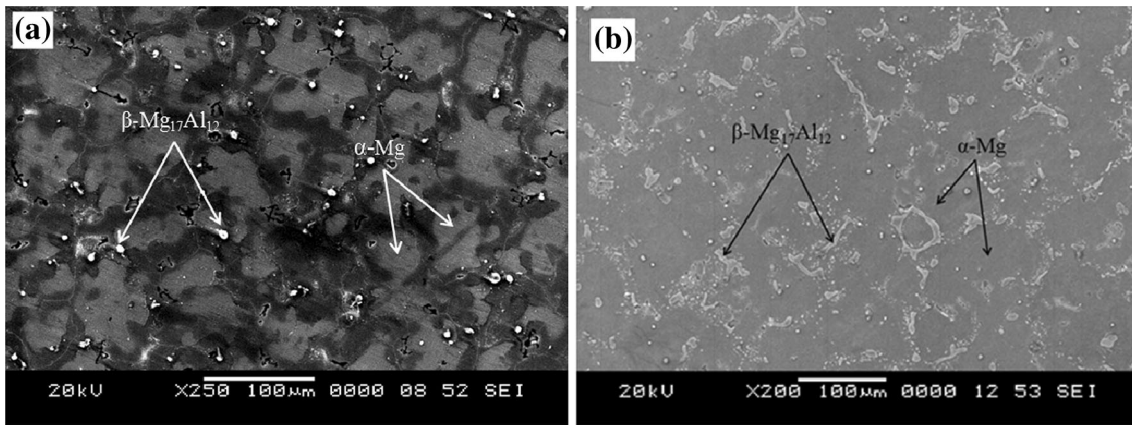


Fig. 2 SEM images of AM70 alloy (a) as-cast sample and (b) homogenized sample

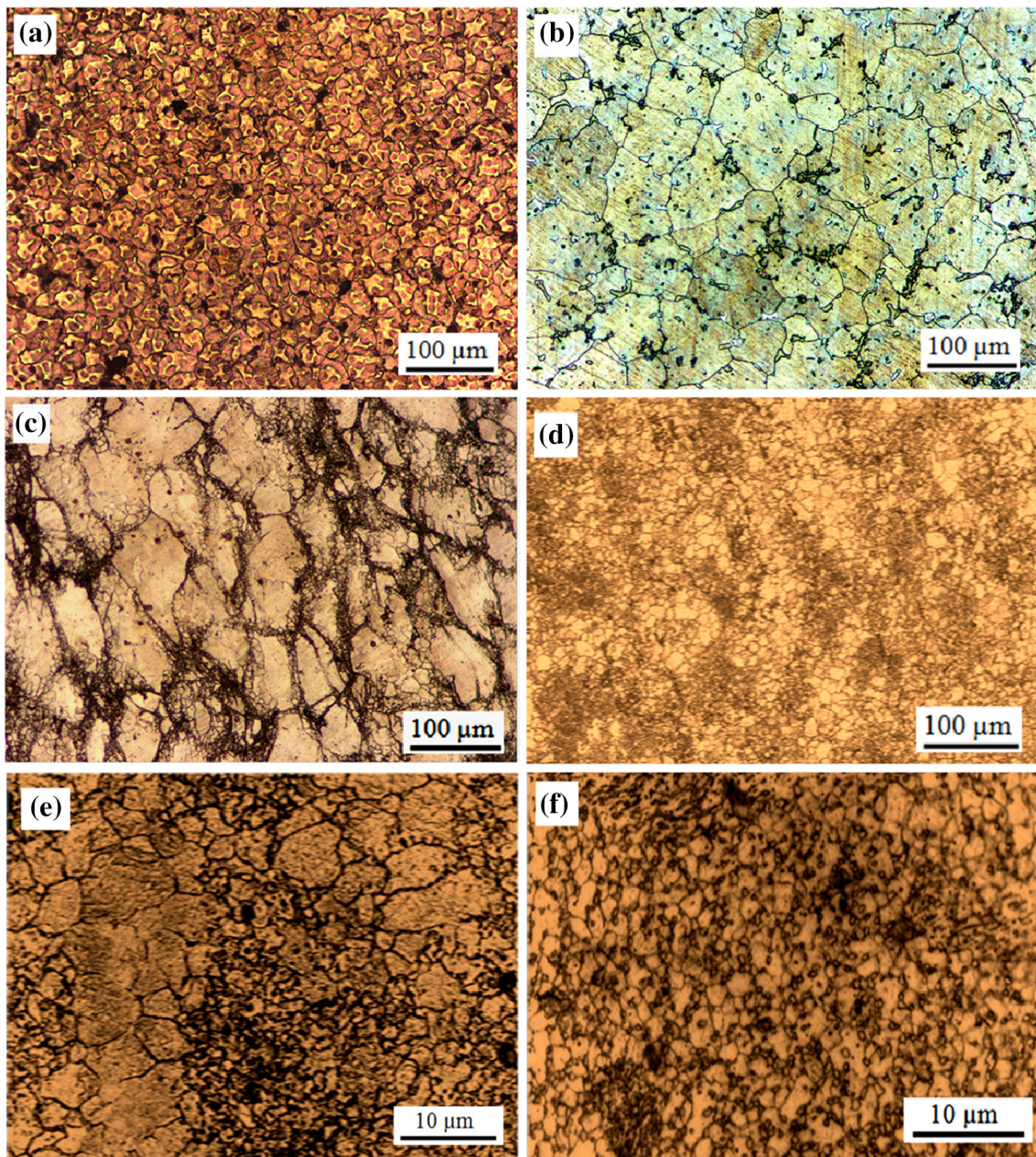


Fig. 3 Optical microstructures of AM70 alloy (a) as-cast, (b) homogenized, (c) 1P, (d) 2P, (e) 3P, and (f) 4P samples

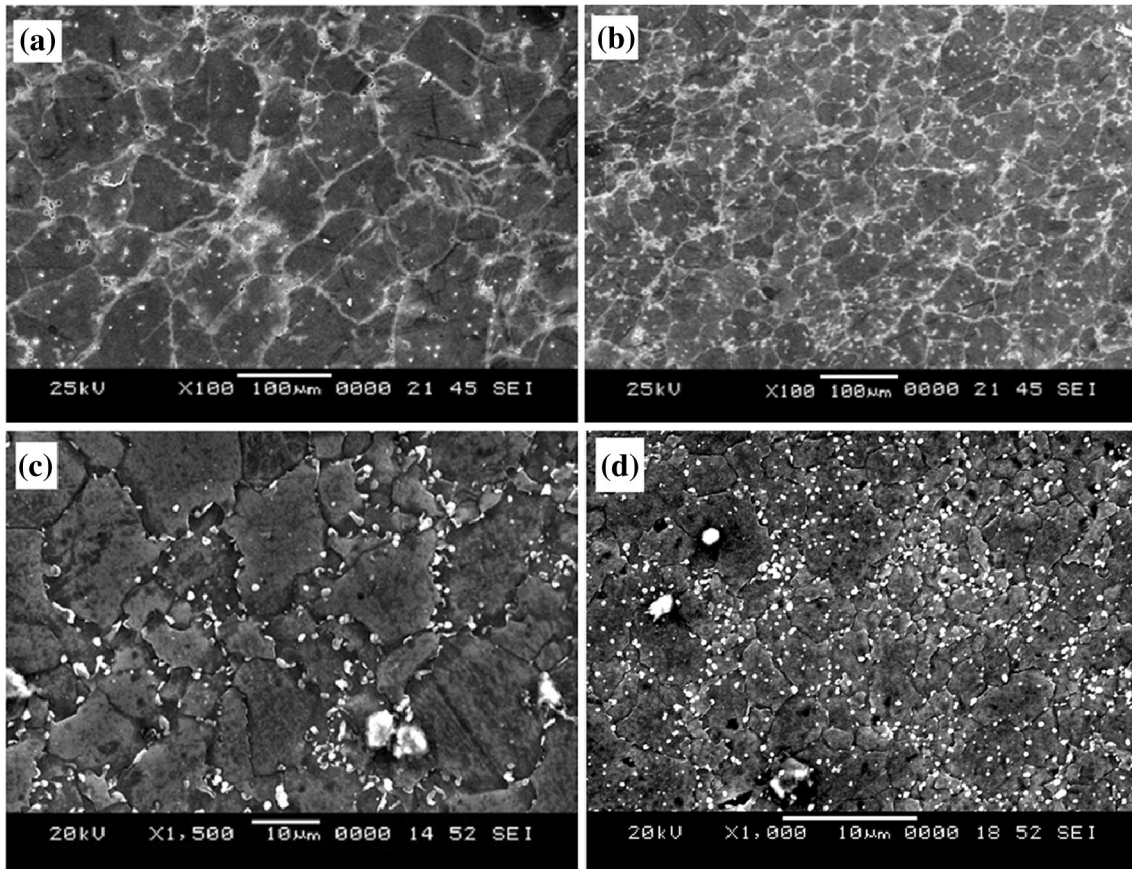


Fig. 4 SEM images of ECAP (a) 1P, (b) 2P, (c) 3P, and (d) 4P samples

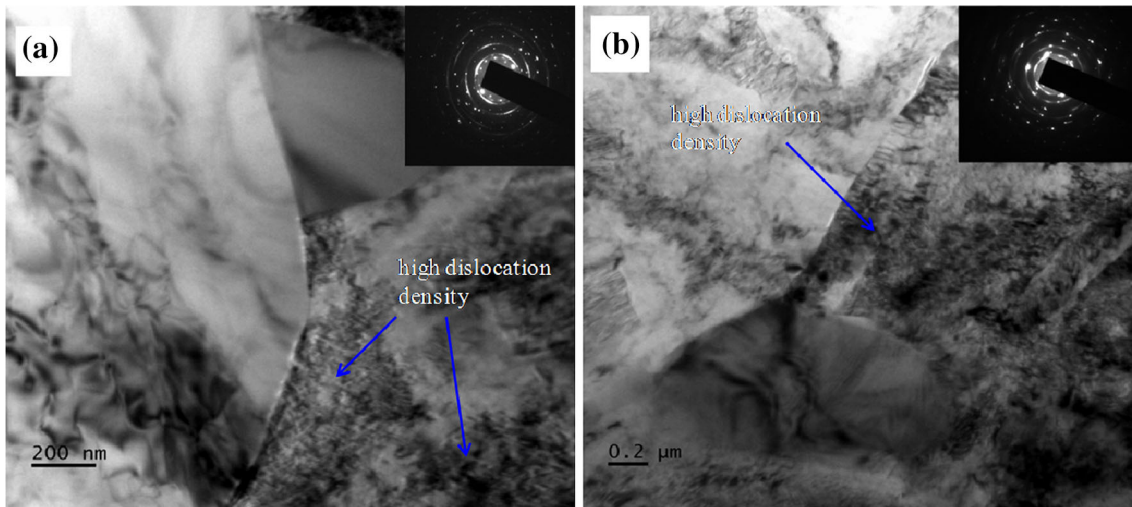


Fig. 5 TEM images of ECAP 4P sample

3. Results and Discussion

3.1 Microstructural Analysis

Figure 2(a) shows the SEM images of the as-cast magnesium alloy AM70. Microstructure consists of α -Mg as the matrix and a large volume of β -Mg₁₇Al₁₂ as the secondary

phase. β phase particles are randomly distributed over the enter matrix and the grain boundaries are not clear. Average grain size of the cast alloy was found to be 45 μ m. The as-cast material was subjected to homogenization treatment at 400 °C for 24 h. During homogenization, secondary β phase particles dissolved in the matrix and the traces of the secondary phase are seen along the grain boundaries. Grain boundaries are

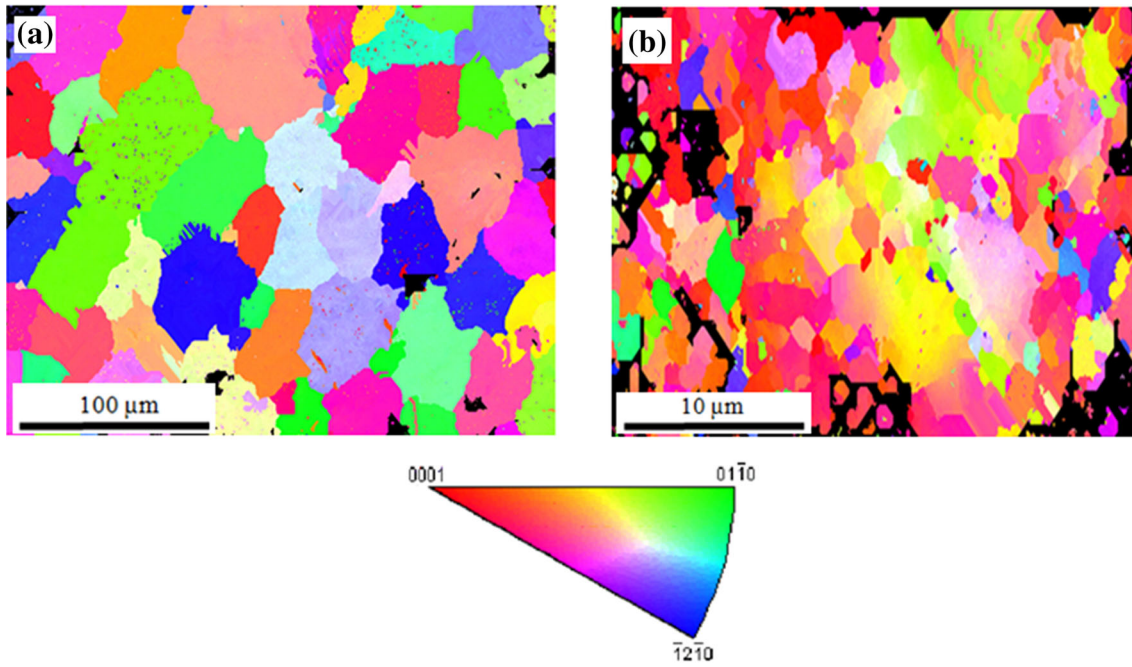


Fig. 6 OIM with IPF image (a) as-cast and (b) ECAP 4P samples

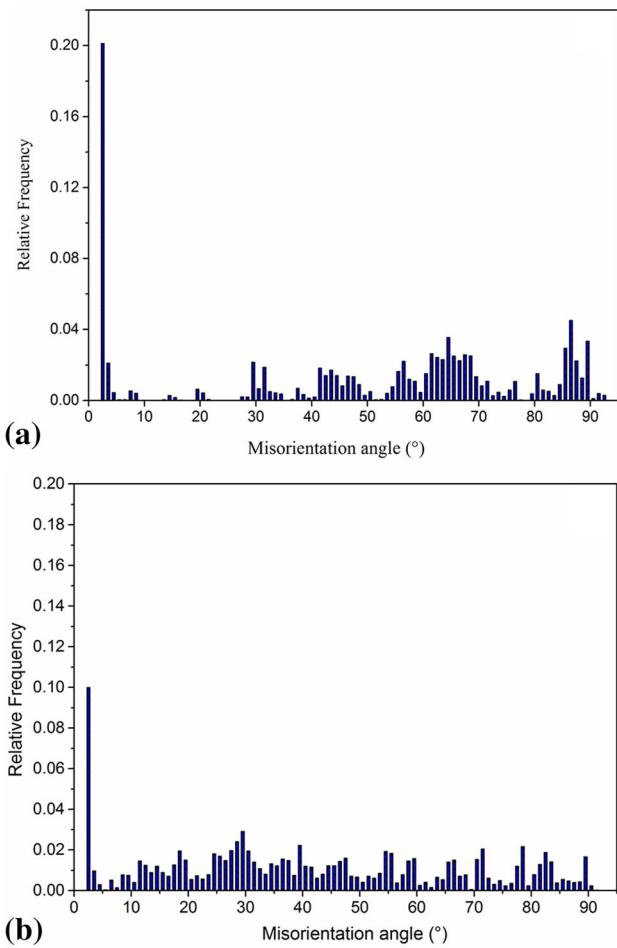


Fig. 7 Misorientation angles of (a) as-cast and (b) ECAP 4P samples

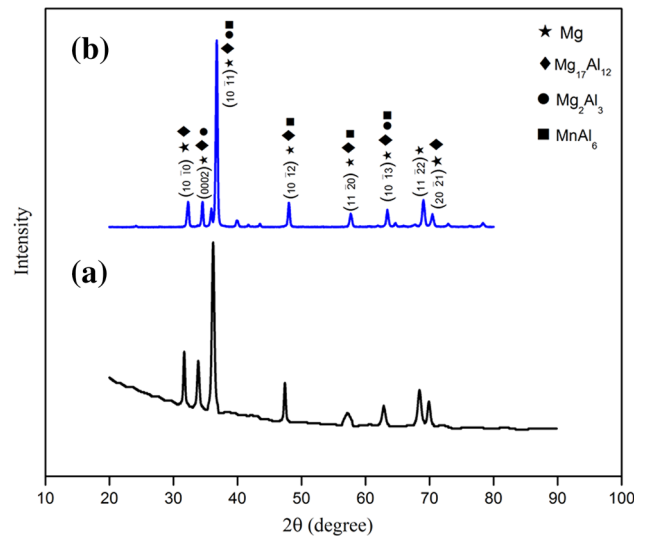


Fig. 8 XRD patterns of (a) as-cast and (b) ECAP 4P samples

clearly visible; thus, each grain can be distinguished. Average grain size of the homogenized material (Fig. 2b) was found to be 100 μm . The increase in grain size is because of static recrystallization process which happened during homogenization treatment.

Homogenized samples were subjected to ECAP processing for up to 4 passes. During the 1 pass, initial coarse grains are broken into too many fine grains in such a way that smaller grains are encircled by larger grains, which leads to heterogeneous bimodal microstructure of material as shown in Fig. 3(a). More grain refinement occurs during initial passes, which is due to high rate of dislocations generation. Grains are bimodal after first ECAP pass with some large grains of size 55 to 65 μm surrounding the arrays of small grains of size 30 to 35

μm . The average grain size in the entire microstructure after first pass was found to be $60\ \mu\text{m}$. Further grain refinement occurs during the ECAP 2, 3, and 4 passes. It is clear from Fig. 3(d) and (f) that homogeneous and refined grain size microstructure is obtained after 2, 3, and 4 ECAP passes. Grain size after 4 pass was found to be an average of $1\ \mu\text{m}$. Reasonable homogeneity and equiaxed microstructure at higher passes may be due to dynamic recrystallization (DRX) occurring during ECAP processing or static recrystallization prior to the ECAP processing, i.e., during heating to reach the desired temperature.

Figure 4(a) and (d) shows the SEM images of ECAP-processed samples from 1 to 4 passes. In Fig. 4(b), second-phase particles can be found in a great proportion at grain boundaries, but inside the grain, most of the surface is free of particles. Figure 4(c) and (d) shows the microstructure of 3 and 4 pass samples. The average grain size analyzed from the microstructure came to be 8 and $1\ \mu\text{m}$ for 3 pass and 4 pass samples, respectively. This grain refinement is due to DRX during ECAP processing (Ref 15). The presence of various phases in the ECAP-processed samples has been separately discussed under “X-ray Diffraction Analysis” section in this manuscript.

Figure 5(a) and (b) shows the TEM images with selected area electron diffraction (SAED) patterns (at inset) of ECAP 4 pass sample. Existence of high dislocation density is observed in the microstructure. Diffraction spots from SAED patterns are in the form of rings, indicating large fraction of HAGBs. Few diffraction spots are separated and do not form rings, which may be due to the presence of LAGBs. Some diffraction spots look stretched or elongated, which indicates the presence of high internal stress due to diffusion of some grain boundaries which are in high energy states (Ref 17).

Orientation imaging microscopy (OIM) with the inverse pole figure (IPF) map is shown in Fig. 6. Colors present in IPF map represent the different crystal orientations. The as-cast alloy shows a heterogeneous structure, but fine and equiaxed grains are seen in ECAP-processed 4 pass sample. Distribution of grain boundaries is observed with clear increase in misorientation angles for ECAP 4 pass sample in comparison to the as-cast sample as shown in Fig. 7. Strong peaks were observed in both as-cast and ECAP 4 pass sample in low angle area ($<5^\circ$) and dispersed groups of peaks were observed at higher angles. Increase in misorientation angle of the grain boundaries for ECAP 4 pass sample in comparison to as-cast sample can be observed in the angle range from 10° to 60° . From Fig. 4(c) and (d), it was observed that grain refinement rate reduced at higher number of ECAP passes when compared to initial pass. Also, by increasing the strain (i.e., by increasing the number of ECAP passes), a transition from LAGBs to HAGBs occurs, leading to a more stable microstructure. This happens due to DRX occurring on the grain boundaries (Ref 17). With increase in number of ECAP passes, frequency of HAGBs increased. Even though, the frequency of LAGBs decreased with an increase in HAGBs during higher number of ECAP passes, not much change in grain size was observed. Fraction of recrystallized grains increased with increase in strain due to the higher rate of nucleation of new grains during recrystallization, which resulted in a relatively uniform microstructure with ultrafine grains as shown in Fig. 3(f) and 4(d). Obtained results show that much grain refinement takes place during initial stages of ECAP and higher deformation produces more HAGBs.

3.2 X-ray Diffraction Analysis

Figure 8 shows the x-ray diffraction (XRD) patterns of as-cast and ECAP-processed 4 pass samples. It was noticed that the planes $(10\bar{1}0)$, (0002) , and $(10\bar{1}2)$ for as-cast material show a strong trend of intensity, while no such tendency occurred after ECAP 4 pass. Intensity of plane $(10\bar{1}1)$ increased after ECAP 4 pass, but much decrease in intensity was observed for $(10\bar{1}0)$ plane. These changes are due to grain refinement occurring during ECAP processing. From Fig. 8, it can be seen that a strong texture is observed for as-cast sample and this texture decreases for ECAP 4 pass sample. Shear deformation which took place during the ECAP processing eliminated the existing texture and due to that, the intensity of texture decreased with increase in number of ECAP passes. As the ECAP passes increased, the initial texture was completely removed and in the meantime, shear deformation by ECAP gave rise to new texture.

3.3 Mechanical Properties

3.3.1 Tensile Behavior. Tensile tests were carried out for the as-cast, homogenized, and ECAP-processed samples and the obtained results are shown in Fig. 9. From the plot, it is

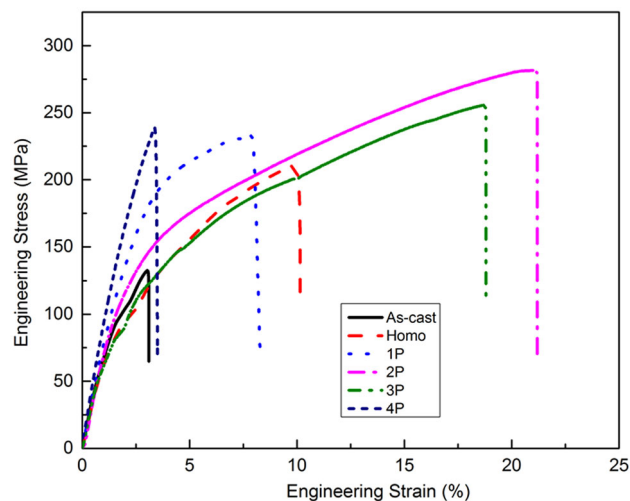


Fig. 9 Tensile properties for as-cast, homogenized, and ECAP-processed samples

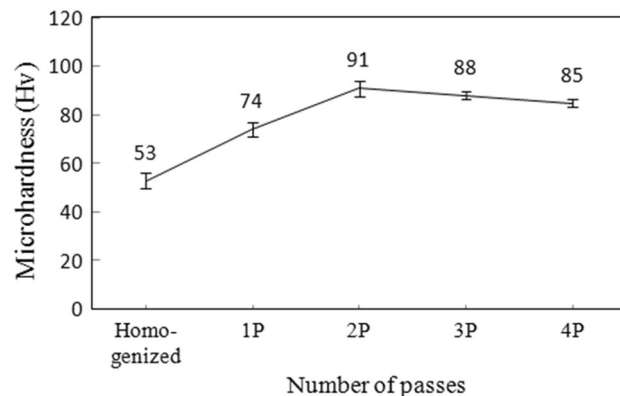


Fig. 10 Microhardness of homogenized and ECAP-processed samples

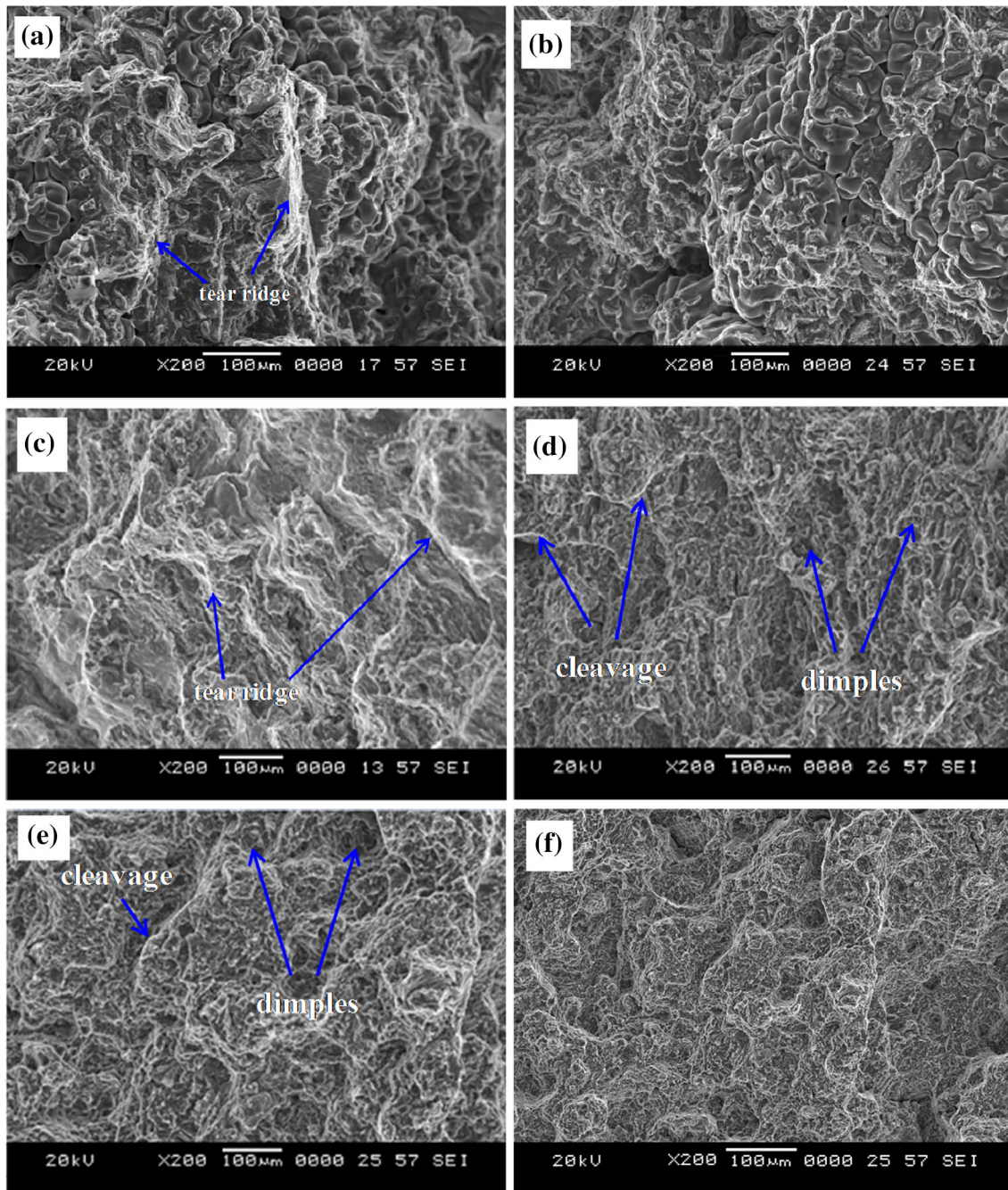


Fig. 11 SEM images of fracture surfaces (a) as-cast, (b) homogenized, (c) 1P, (d) 2P, (e) 3P, and (f) 4P samples

observed that ultimate tensile strength (UTS) increased up to 2 passes but decreased with further ECAP passes. UTS of 2 pass ECAP-processed sample was 282 MPa, which is 212 and 134% larger as compared to the UTS of as-cast (133 MPa) and homogenized sample (210 MPa). After 2 passes, elongation was 20.7%, while it was 3.1% for the as-cast sample. UTS obtained for 3 pass and 4 pass samples were 255 and 242 MPa, respectively. Yield strength (YS) obtained for 2 pass ECAP sample was 170 MPa, which is 288 and 179% larger as compared to YS of as-cast sample (59 MPa) and homogenized sample (95 MPa). YS obtained for 3 pass and 4 pass samples are 135 and 120 MPa, respectively. Increase in UTS is due to grain boundary strengthening mechanism according to which

reduced grain size leads to increased UTS as explained by Hall-Petch equation (Ref 18). It may also be due to the increment in precipitation of intermetallic phases in the matrix of the material as shown in Fig. 8. Maximum UTS was observed for 2 pass sample (as shown in Fig. 9), i.e., the grain refinement rate was maximum for this sample. The deviation in the UTS of various ECAP-processed samples may be firstly, due to a decrement in grain refinement rate as seen in Fig. 3(e) and (f). Secondly, it may be due to DRX that happened during ECAP processing which led to the elimination of dislocations and also because of static recrystallization prior to ECAP processing.

Thirdly, even though the grain size of ECAP-processed material decreased, there was a reduction in UTS which may be

because of texture modification that happened in HCP structure of magnesium. ECAP processing modified the initial texture and grain size of the material simultaneously as observed from the variation in intensities on comparing as-cast and ECAP 4 pass sample as shown in Fig. 8. Fluctuations in the intensity of planes were observed for peaks (10 $\bar{1}$ 0), (10 $\bar{1}$ $\bar{1}$), (10 $\bar{1}$ 2), (11 $\bar{2}$ 0), (10 $\bar{1}$ 3), (11 $\bar{2}$ 2), and (20 $\bar{2}$ 1) including the basal plane (0002). This behavior shows that there is a change in texture during the ECAP processing with the activation of prismatic and pyramidal slip, which might have been influenced by the generation of new grain boundaries. Due to limited slip systems of Mg alloys, strength is greatly influenced by texture modification and slip usually takes place on basal planes. Strength increases with a decrease in the grain size only up to a certain limit, if texture remains constant (Ref 14). A characteristic feature of ECAP-processed samples is their enhanced ductility as compared to the as-cast condition. This is due to strain hardening effect occurring in the material. Finally, we observe from Fig. 9 that even though there was a decrease in UTS after 2 passes, the UTS and YS of 3 pass and 4 pass samples held quite high values as compared to as-cast and homogenized samples.

3.3.2 Vickers Microhardness. Vickers microhardness test was carried out across the cross-section to check the uniformity in hardness throughout the ECAP-processed samples. Figure 10 illustrates the relation between microhardness value (Hv) and number of ECAP passes. With an increase in the number of ECAP passes, microhardness value increased from 53 Hv for homogenized sample to a maximum of 91 Hv for 2 pass sample which is due to strain hardening effect. But with further ECAP passes, a slight reduction in microhardness values was observed. It is due to formation or nucleation of new grains which obstructs the effect of strain hardening. Uniformity of microhardness for 1 pass and 2 pass samples is less compared to 3 pass and 4 pass sample. Enhancement in uniformity of microhardness with increasing ECAP passes is because of homogeneous microstructure in the 3 pass and 4 pass sample.

Variation in microhardness is related to the ultimate tensile strength and has found to be interdependent on each other. Figure 3 and 4 show that grain size decreased with higher passes and also Fig. 10 implies that microhardness decreased after 3 ECAP passes. A similar trend was observed for UTS (Fig. 9), too. This shows that ECAP-processed samples do not have the same texture throughout the material as observed through XRD results (as shown in Fig. 8). Relation between hardness and grain size can be explained by the Hall-Petch equation (Ref 18).

3.4 Fractography

SEM images of fracture surfaces (after tensile test) of the as-cast, homogenized, and ECAP-processed 1, 2, 3, and 4 pass tensile specimens are shown in Fig. 11. Tearing ridges are visible on the fracture surface of as-cast, homogenized, and 1 pass ECAP-processed sample as shown in Fig. 11(a) and (c) which are due to plastic deformation of the material. For the 2 pass sample, cleavage planes are observed as shown in Fig. 11(d). The frequency of cleavage planes decreased as grain size reduced with higher number of ECAP passes and fewer cleavage planes were observed on the fracture surfaces for ECAP 4 pass sample. Initially, it looked like a mixed mode of ductile and brittle fracture. After 2 passes, fracture surface

with high fraction of fine and equiaxed dimples is observed, which are nearly homogeneous in size and represent the features of ductile fracture.

4. Conclusions

An investigation of microstructure and mechanical properties of AM70 magnesium alloy processed by ECAP was carried out and the following conclusions are summarized based on the obtained results:

- AM70 alloy was successfully processed by ECAP up to 4 passes at 275 °C using route B_C. The grain size reduced to an average of 1 μm. Initially, the microstructure was bimodal and as the number of ECAP passes increased, homogeneous structure was observed. Dynamic recrystallization was found to be the mechanism for grain refinement. EBSD results showed that frequency of HAGBs increased with increase in strain rate.
- UTS increased up to 2 passes of ECAP processing, which came 212 and 134% larger as compared to that of as-cast and homogenized samples, respectively. Increase in UTS is attributed to grain boundary strengthening mechanism. YS increased up to 2 passes of ECAP processing, which came 288 and 179% larger as compared to that of as-cast and homogenized samples, respectively. Ductility for ECAP 2 pass sample came 20.7%, while it was just 3.1% for the as-cast sample. With further ECAP passes, strength and ductility reduced but the obtained results still held higher values as compared to that of as-cast condition.
- Hardness increased up to ECAP 2 pass and decreased with further passes. Hardness exhibited the same trend as UTS; thus, the two test results seemed to be interdependent on each other. Nonuniformity in hardness values across the cross-section was found to be due to strain hardening effect.
- Fracture surface of ECAP-processed alloy showed fine and equiaxed dimples type of fracture, which signify ductile fracture behavior.

References

1. M.K. Kulekci, Magnesium and its Alloys Applications in Automotive Industry, *Int. J. Adv. Manuf. Technol.*, 2008, **39**(9), p 851–865
2. Y. Kojima, *Handbook Advanced Mg Technology*, Kallos Publishing Co., Ltd., Tokyo, 2000
3. J. Chapman and D. Wilson, Room-Temperature Ductility of Fine-Grain Magnesium, *J. Inst. Met.*, 1962, **91**(1), p 39–40
4. R.Z. Valiev, Y. Estrin, Z. Horita, T.G. Langdon, M.J. Zechetbauer, and Y.T. Zhu, Producing Bulk Ultrafine-Grained Materials by Severe Plastic Deformation, *JOM*, 2006, **58**(4), p 33–39
5. W. Chen, D. Ferguson, and H. Ferguson, Severe Plastic Deformation Techniques, *Acta Metall. Sin.*, 2009, **13**(1), p 242–253
6. T.C. Lowe and R.Z. Valiev, The Use of Severe Plastic Deformation Techniques in Grain Refinement, *JOM*, 2004, **56**(10), p 64–68
7. Y. Estrin and A. Vinogradov, Extreme grain Refinement by Severe Plastic Deformation: A Wealth of Challenging Science, *Acta Mater.*, 2013, **61**(3), p 782–817
8. Azushima, R. Kopp, A. Korhonen, D.Y. Yang, F. Micari, G.D. Lahoti, P. Groche, J. Yanagimoto, N. Tsuji, A. Rosochowski, and A. Yanagida, Severe plastic deformation (SPD) processes for metals, *CIRP Ann. Manuf. Techn.*, (2008), **57**(2), p 716–735

9. R.Z. Valiev and T.G. Langdon, Principles of Equal-Channel Angular Pressing as a Processing Tool for Grain Refinement, *Progr. Mater. Sci.*, 2006, **51**(7), p 881–981
10. R.B. Figueiredo, P.R. Cetlin, and T.G. Langdon, The Processing of Difficult-to-Work Alloys by ECAP with an Emphasis on Magnesium Alloys, *Acta Mater.*, 2007, **55**(14), p 4769–4779
11. Q. Yang and A.K. Ghosh, Deformation Behavior of Ultrafine-Grain (UFG) AZ31B Mg Alloy at Room Temperature, *Acta Mater.*, 2006, **54**(19), p 5159–5170
12. K. Watanabe, K. Matsuda, T. Gonoji, T. Kawabata, K. Sakakibara, Y. Sanpei, S. Saikawa, and S. Ikeno, Effect of Casting Method and Al Contents on Microstructure in AM-Type Magnesium Alloys, *Mater. Sci. Forum*, 2010, **654-656**, p 656–663
13. O. Kulyasova, R. Islamgaliev, B. Mingler, and M. Zehetbauer, Microstructure and Fatigue Properties of the Ultrafine-Grained AM60 Magnesium Alloy Processed by Equal-Channel Angular Pressing, *Mater. Sci. Eng. A*, 2009, **503**(1-2), p 176–180
14. F. Akbaripanah, F. Fereshteh-Saniee, R. Mahmudi, and H.K. Kim, Microstructural Homogeneity, Texture, Tensile and Shear Behavior of AM60 Magnesium Alloy Produced by Extrusion and Equal Channel Angular Pressing, *Mater. Des.*, 2013, **43**, p 31–39
15. F. Akbaripanah, F. Fereshteh-Saniee, R. Mahmudi, and H.K. Kim, The Influences of Extrusion and Equal Channel Angular Pressing (ECAP) Processes on the Fatigue Behavior of AM60 Magnesium Alloy, *Mater. Sci. Eng. A*, 2013, **565**, p 308–316
16. F.D. Dumitru, O.F. Higuera-Cobos, and J.M. Cabrera, ZK60 Alloy Processed by ECAP: Microstructural, Physical and Mechanical Characterization, *Mater. Sci. Eng. A*, 2014, **594**, p 32–39
17. V.V. Stolyarov, Y.T. Zhu, I.V. Alexandrov, T.C. Lowe, and R.Z. Valiev, Influence of ECAP Routes on the Microstructure and Properties of Pure Ti, *Mater. Sci. Eng. A*, 2001, **299**(1), p 59–67
18. T. Nieh and J. Wadsworth, Hall-Petch Relation in Nanocrystalline Solids, *Scripta Metall. Mater.*, 1991, **25**(4), p 955–958